Optimization of UAV-Fixed Wing for Topographic Three Dimensional (3D) Mapping in Mountain Areas

Hendra Saputra[1], Faisal Ananda[2] , Galih Prasetya Dinanta[3], Awaluddin[4], Edward[5]

{hendrasaputra@polbeng.ac.id[1] , anandabrawijaya@gmail.com[2], gali006@brin.go.id[3], awal004@brin.go.id[4], edward.dishub@gmail.com[5]}

Bengkalis State of Polytechnic, Riau, Indonesia[1,2].
Research Center for Remote Sensing, Research Organization for Aeronautics and Space, National Research and Innovation Agency, Indonesia[3,4].
Regional Development Planning Board, Anambas, Indonesia[5]

Abstract. This study aims to produce a 3D terrain visualization from the Digital Terrain Model from UAV-Fixed Wing data. In this study, data acquisition was performed by utilizing a Fixed Wing UAV equipped with a Sony Alpha 6000 camera. The study area is a predominantly hilly area, with a height approximately up to 327 meters from mean sea level. as part of acquisition process, the flight mission planning was rigorously designed by using the Mission Planner software. A total of six flying missions were conducted to collect the necessary aerial photo data. In addition, Aerial photo data is processed by generating photo ortho mosaics through the Structure from the Motion Photogrammetry technique. Ground Control Points (GCP) and Independent Check Points (ICP) are integrated with in the process to enhance data accuracy and precision. ICP has an essential role as a verification tool, ensuring the conformity of the geometric position of the map with the actual coordinates on the earth's surface. The results of this study are Digital Terrain Model (DTM) data which is represented in a three-dimensional topography visualization. Subsequently, Raster data from DTM can be incorporated with BIM-based software, such as Autodesk Infraworks, where it more applicable for advanced planning and design. the results of this study discover that the accuracy of horizontal and vertical positions complies with the established standards as stated by Geospatial Information Agency Regulation Number 6 in 2018, where the 1:10,000 scale map have class 1 horizontal accuracy and class 3 vertical accuracy.

Keywords: Fixed Wing UAV, 3D Terrain, Digital Terrain Model (DTM)

1 Introduction

In recent years, Unmanned Aerial Vehicles (UAVs) or commonly called drones, have garnered immense popularity and attention. Many studies highlight multi-rotors UAV due to, their

prominence with straightforward control mechanisms and exceptional precision in positioning[1]. Mountain areas are characterized by rugged and complex terrain. Hence, it poses challenges for UAV flight and navigation [2]. The ruggedness of uneven terrain, combined with the challenges posed by steep inclines and constricted valleys, frequently contribute to stability of fixed-wing UAVs and affects the ability to navigate properly around obstacle. Low air pressure and strong winds are atmospheric factors on mountainous terrain, which can be affected by the stability and control of UAVs [3]. Therefore, The environmental conditions present in the area can make it difficult to determine a precise, accurate and effective position on each flight path of a fixed-wing UAV system.Some researchers, including [4] have studied the use of UAVs for 3D topographic mapping. where the research site he used in his publication covered two different areas: flatlands and hilly terrains with elevations ranging from 70 to 80 meters above sea level. To generate the DEM of this terrain, eight interpolation techniques were employed: Kriging, Natural Neighbors, Triangulation with Radial Basis Function accompanied by Linear interpolation, Nearest Neighbors, Inverse Distance Weighting, Local Polynomial, and Minimum Curvature. Meanwhile, in this research, the study area focuses on a hilly region with an elevation of approximately 327 meters above Mean Sea Level (MSL). This area spans roughly 843.21 hectares. A Digital Terrain Model (DTM) is generated through a photogrammetry process known as Structure from Motion to map the region's topography.

The current research is primarily focused on understanding the horizontal and vertical accuracy of orthophotos produced by fixed-wing unmanned Aerial Vehicles (UAVs). The significant elements of this study was to ensure that the results of orthophoto images preserve a high degree of precision, both in horizontal and vertical perspectives. Simultaneously, this study aims to thoroughly examine the methods to achieve an optimal three-dimensional contour visualization, assuring that these contours accurately reflect the observed land surface.

In addition, this study explores the potential of integrating point cloud data obtained from Fixed Wing UAVs with applications based on Building Information Modeling (BIM). With such integration, the utilization of UAV-derived data within BIM applications can be optimized, which can potentially contribute to enhance the processes of planning, design, and execution in construction projects. A key objective of this research is to assess the compatibility and effectiveness of merging point cloud data from the Fixed Wing UAV with BIM-oriented applications

This study attempt to generate 3D terrain visualization from the Digital Terrain Model from UAV-Fixed Wing data. This research contributes to time efficiency and low cost in generating accurate and comprehensive 3D topography visualizations.

2 Study Site

Tarempa City is part of the administrative area of Anambas Islands Regency, Riau Archipelago Province, Indonesia. The area of aerial photo acquisition is ± 843.21 Ha, which mainly covers the Siantan District, Anambas Islands Regency. The terrain condition in Siantan District tends to be hilly, with the highest elevation of ± 450 m above mean sea level.
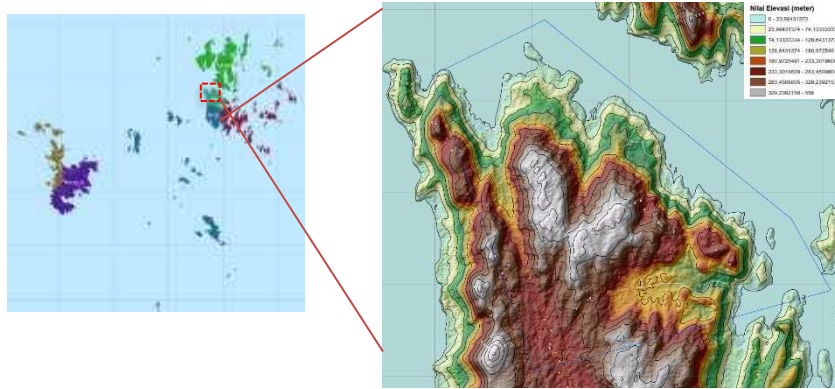
Fig. 1. Location of Study.

3 Research Method

Fig. 2. Flowchart of Methodology

3.1 Flight Mission

Flight mission plans were created using the Mission Planner software. Before data acquisition, various parameters, such as pixel size, flight altitude, photo overlap (front lap/side lap), camera sensor specifications, speed, and other factors, were required as inputs. The Siantan District mapping covered six flying missions, the details of which are presented in Figure 3.
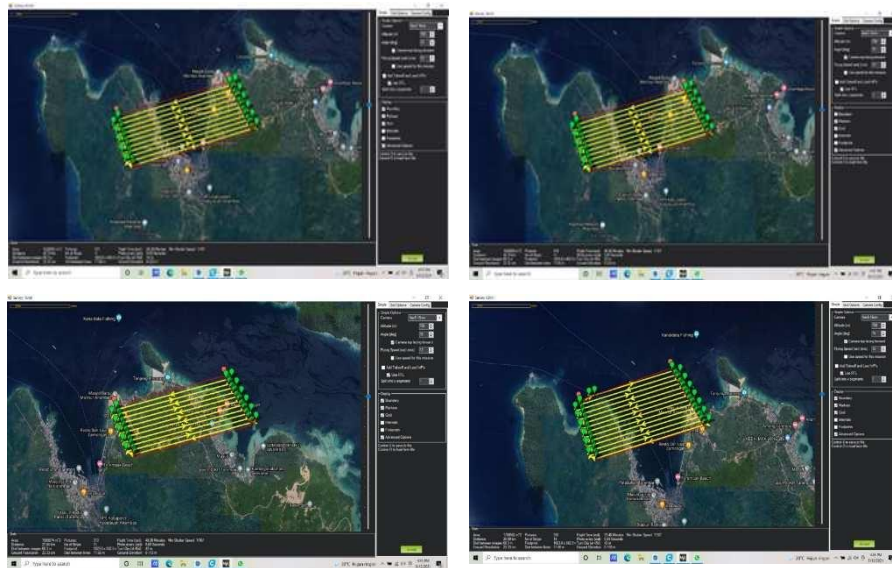
Fig. 3. Flight Mission of UAV Fixed-Wing (Mission Planner Software)

The input parameters in the mission planner software include Flying Height 700 Meters from MSL, Frontlap/Sidelap 80/70%, Camera Model ILCE – 6000, Resolution 6000 x 4000, and Focal Length 20 mm.

3.2 Ground Control Point (GCP) and Independent Check Point Distribution (ICP)

The planning for Ground Control Points (GCP) and Independent checkpoints (ICP) was conducted using ArcMap. Ideally, GCP tie points should be evenly distributed across the imaging area. The placement of GCPs should represent various topographic configurations and relief. GCPs are essential for photogrammetry software's block bundle adjustment process, converting the point cloud coordinates from model coordinates to their actual field counterparts. On the other hand, ICPs are field coordinates used to test the accuracy of the orthophotos and the Digital Surface Model (DSM) generated from aerial photo processing. A map illustrating the distribution of GCPs is presented in Figure 4.

Fig. 4. Applying and Measurement of GCP and ICP

3.3 Measurement of Coordinates GCP and ICP

Measurement of Ground Control Points (GCP) coordinates is a essensial step that performed after installing all GCP (X) markers in the field. the Trimble R8s Geodetic GNSS is used to make these measurement, which is known to provide a high precision in reading. The instrument's accuracy is quite impressive, with the ability to measure every point down to the centimeter level and, in some conditions, even millimeters. Of course, this accuracy is greatly influenced by the method used and the duration of the observation. GCP measurements are carried out using the Real Time Kinematic (RTK) method. The RTK method is not a new method in the world of geodesy, but it remains one of the favorite by experts due to its several advantages. One of its advantages is time efficiency, where it capable to measures accurate results in a relatively short time. As a reference point, measurements are made using the CORS BIG-Ranai Station, Natuna (RTCM 0089), known for its high standards of accuracy, this expected to obtain reliable measurement results. With a combination of modern equipment and appropriate measurement methods, it can be expected that the data obtained from these GCP measurements will significantly contribute to increasing the accuracy of mapping and other geospatial analyses.
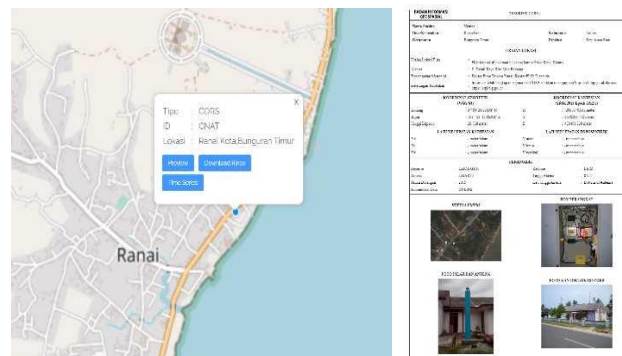
Fig. 5. CORS Station of BIG, Ranai, Natuna Regency

Location of Cors BIG Station in Ranai City, Natuna Regency. Code and coordinates of the Cors Ranai station RTCM 0089, X = 876303.843, Y = 436384.57, Z = 26.729 (meters). The description of the Cors Ranai station is presented in the image below.

3.4 Acquisition of Aerial Image

Aerial photo acquisition was conducted using a Fixed Wing UAV. This Fixed Wing UAV was chosen due to the study location on the coast of the South China Sea, an area known for strong winds. The fixed-wing UAV has a wingspan of 2.2 meters, a length of 1.2 meters, and a weight of 6 kg, and it can fly for about 1 hour. Additionally, this UAV is equipped with a Sony Alpha 6000 camera. The fixed-wing UAV is shown in Figure 1

Fig. 6. UAV Fixed Wing

4   UAV Data Collection and Processing

4.1 Geotagging Data

Geotagging is the process of registering the coordinates generated from the GPS of a Fixed Wing UAV to the corresponding aerial photos. When the UAV initially captures these photos, they do not contain any coordinate information. As a result, for creating an ortho-mosaic, a detailed and accurate composite image — geotagging must be performed as an essential preliminary step. The aerial photo geotagging process in the mission planner is shown in Figure 7
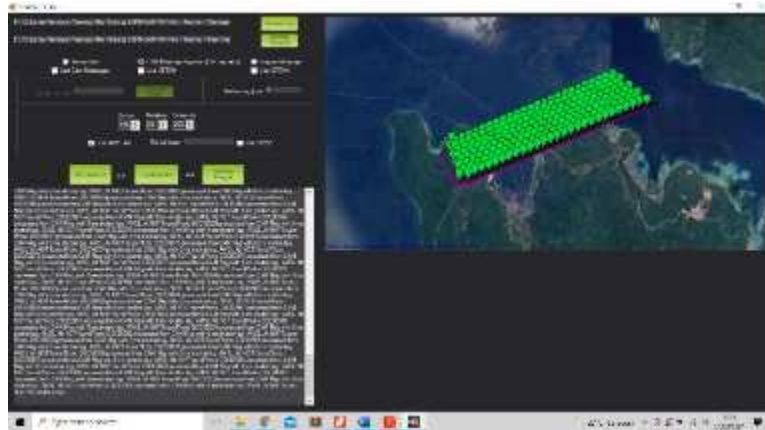
Fig. 7. Aerial photo geotagging process

The method used for geotagging aerial photographs with a mission planner involves utilizing the CAM Message from the data log. This method allows the camera to be triggered during pre-programmed missions or through remote control activation using the DO_DIGICAM_CONTROL or DO_SET_CAM_TRIGG_DIST commands. Corresponding CAM messages are then stored in the data flash log and can be utilized by the Mission Planner to add accurate geotag information to the images.

4.1 Build Aligning

Photo alignment is carried out to identify points within each photo and to match identical points across two or more photos. This process of photo alignment produces an initial 3D model, positions of the camera and photo for each shot, and a sparse point cloud, which will be utilized in the subsequent stage. Aligning in Agisoft Metashape Processing in Figure 3
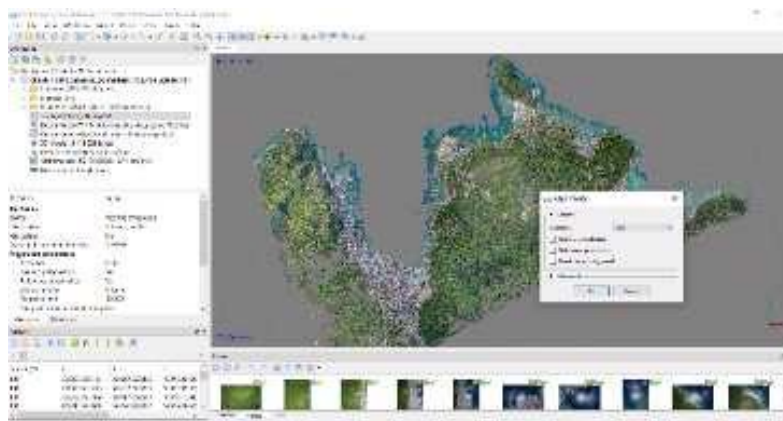
Fig. 8. Aligning in Agisoft Metashape Processing

4.2 Georeferencing Ground Control Point

Ground control points are required to do the image orientation [5]. This study uses 10 Ground Control Points. The GCP coordinates are measured using the Trimble R8s Geodetic GNSS using the RTK-NTRIP method. It is recommended that the GCP be installed and distributed evenly in the study area so that the data produced has good precision and accuracy. Georeferencing GCP in Agisoft Metashape Processing is shown in Figure 4.

Fig. 9. Georeferencing GCP in Agisoft Metashape Processing

Based on the illustration provided, it is evident that the inclusion of Ground Control Points (GCP) significantly enhances the accuracy of measurements. Compared to scenarios without GCP, the data obtained with their use is noticeably more precise and consistent [6], [7]. This underscores the important role played by GCPs in elevating the quality and reliability of the data. Thus, employing GCPs can be considered as an essential factor in measurement processes, especially when aiming for dependable and accurate results.

5   Result and Discussion

5.1 Results of Processing the Coordinates for GCP and ICP

From the geodetic GNSS data analysis, the outputs obtained include coordinates for both Ground Control Points (GCP) and Independent Check Points (ICP). To ensure precision, these coordinates were measured using the RTK-NTRIP method. The CORS Station in Ranai, Natuna District, was employed as the reference point for these measurements. However, it is essential to note that the baseline length between Ranai and Terempa is approximately 241.2 km, which could influence the quality of the data obtained. Despite this potential challenge, the measurement results were reassuring. A solution type labeled as "fixed" indicates that the measured coordinates for both the GCP and ICP are of high quality and accuracy, making them reliable for further analysis. Coordinates of GCP and ICP are shown in Table 1

Table 1. Coordinates of GCP and ICP

Patok	Easting (X)	Northing (Y)	Elevation (Z)	Description
RTCM0089	209903.31	436072.85	26.729	Stasiun CORS BIG-RANAI
BM	635515.012	355556.523	16.43	
GCP.TJG	634811.208	355825.329	25.863	
GCP.TJGLBI	634665.679	356259.165	39.219	
GCP.Lapanganvoly	635237.406	355172.129	40.147	

Patok	Easting (X)	Northing (Y)	Elevation (Z)	Description
GCP.RSUD Tarempa	635483.964	355639.313	17.54	
GCP.Bapeda	635637.711	356258.437	24.772	
GCP.Masjid	635725.618	356798.645	28.782	
GCP.Pantai	636498.661	357235.301	15.648	
GCP.RumahSekda	636497.064	356186.197	115.066	
ICP.1jembatan	635424.844	355321.723	16.772	
ICP.2jembatan	635426.877	355317.144	16.829	
ICP.3LgnTenis	635493.319	355506.704	16.125	
ICP.4tg.bendra	635509.552	355579.765	16.825	
ICP.5jmbtnSP	635488.116	355620.809	16.269	
ICP.6jmbtnSP	635492.77	355620.003	16.325	
ICP.7ujgmasjid	635745.313	356836.815	36.46	
ICP.8ujgmasjid2	635795.298	356901.225	36.39	
ICP.9BatuLpe1	636114.986	356963.478	18.425	
ICP.10BatuLpe2	636127.38	356962.384	18.416	
ICP.11TepilautRS	635370.68	355658.036	16.227	
ICP.12Klenteng1	634718.422	356200.772	30.081	
ICP.12Klenteng2	634724.009	356192.339	30.022	
ICP.14Klenteng3	634725.826	356182.45	30.085	
ICP.15plbhnpelni	635292.43	355710.894	16.149	
ICP.16plbhplni2	635289.505	355703.999	16.304	

5.2 Build of Orthophoto

Orthophotos, derived from photogrammetric applications, seamlessly blend geometry with photorealism. This step makes them beneficial for bith novice and expert operators, offering a precise visual representation of an area [8]. The quality of Orthophoto depends on the flying altitude of the UAV, which affects the photo resolution known as GSD, calibration accuracy and camera orientation, data processing techniques to obtain DTM, and computer performance [9]. In this study, orthophotos were generated by utilizing the Structure from Motion (SfM) Photogrammetry technique, a sophisticated method that allows 3D reconstruction from 2D images. To ensure the accuracy and precision of the resulting orthophotos, this research relies on the use of 10 Ground Control Points (GCP). GCPs are reference points on the earth's surface whose coordinates are known with certainty and are used for calibration and orientation in the process of making Orthophoto.

The next step in this process is the use of build mesh. This mesh is a 3D representation of the object obtained from a collection of points. To get a mosaic-orthophoto, the information used comes from the building mesh that has been built. The process of creating this mesh is based on dense cloud data, which is a collection of very dense and detailed points that represent the surface of an object. In mesh reconstruction, this research uses height field parameters and medium-depth maps. These two parameters play an important role in ensuring the resulting 3D representation is accurate and detailed so that the resulting Orthophoto is of high quality and reliable for various applications. True Orthophoto is shown in Figure 10.

The photogrammetry survey of Tarempa City was conducted using a UAV Fixed Wing platform. This system is equipped with a Sony Alpha 6000 RGB camera that has been calibrated for photogrammetric purposes. The Sony Alpha 6000 camera boasts a feature of a 24.3-megapixel APS-C size sensor. Additionally, the UAV Fixed Wing is outfitted with advanced equipment such as Telemetry RFD 900, GPS Tracking, and a Pixhawk 2.4.8 PX 4 32 Bit Flight Controller.
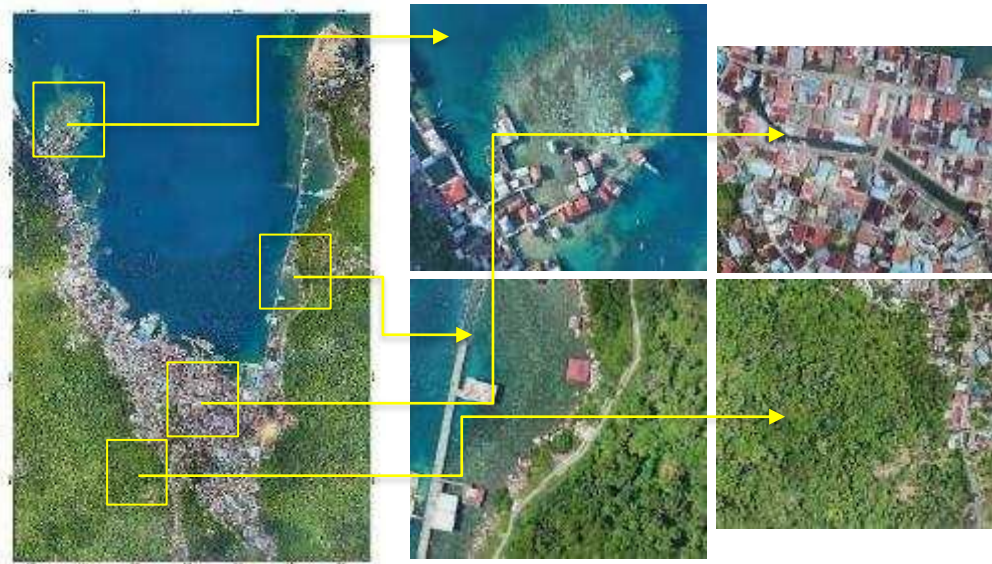
Fig. 10. Orthomosaic Tarempa City.

5.3 Digital Terrain Model

Given the emergence of Unmanned Aerial Vehicles (UAVs) equipped with low-cost digital cameras and better photogrammetric methods for digital mapping, efficient approaches are necessary to allow rapid land surveys with high accuracy [10]. This study produces a Digital Terrain Model (DTM) using the Structure from Motion (SfM) technique. This technique is an approach within the field of photogrammetry that enables the estimation and reconstruction of three-dimensional structures from a series of two-dimensional images [11]. The uniqueness of the SfM technique lies in its ability to estimate these structures by utilizing the sequence of two-dimensional images and information about the movement of the camera or the object in the images. This local motion information, shifts or rotations, is crucial in merging and transforming two-dimensional images into a three-dimensional model. As a result, the DTM produced through the SfM technique can provide a high-accuracy representation of surface topography, which is invaluable for various applications ranging from geomorphological analysis to infrastructure planning [12]. Visualization of Topographic 3D Models is shown in Figure 11
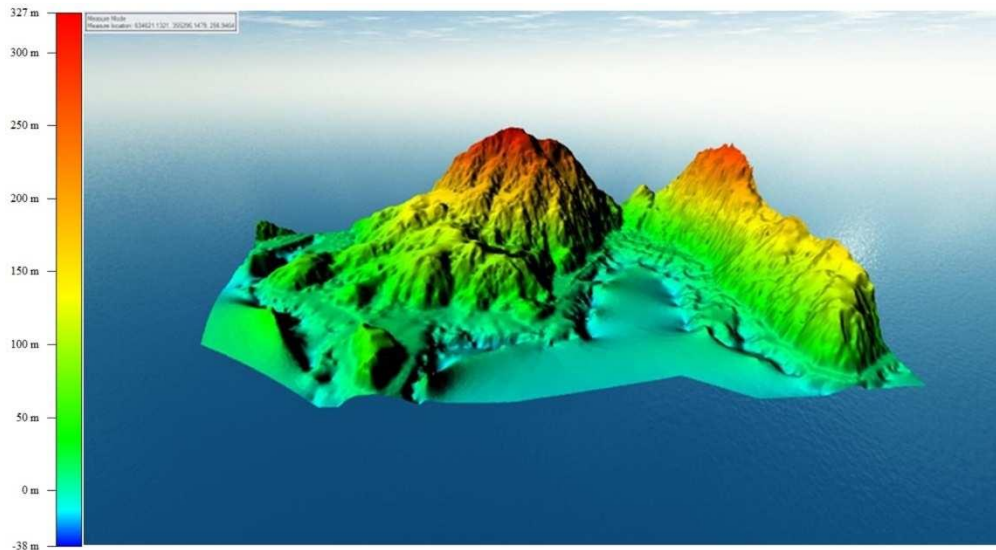
Fig. 11. Visualization of Topographic 3D Models

The picture above indicates that the highest elevation is approximately 327 meters above average sea level, while the lowest elevation is -38 meters. Some researchers say RGB-LED functions as a light emitter, while the image sensor (IS) acts as a receiver. Water turbidity, mainly caused by chlorophyll concentration, can significantly affect light transmittance in the visible spectrum [13]. The Cross Section of the Digital Terrain Model is shown in Figure 12
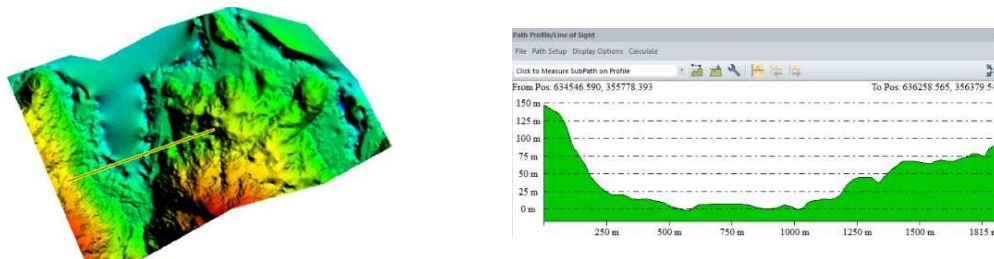
Fig. 12. Cross Section of Digital Terrain Model.

Geographic Information Systems (GIS) and Building Information Modeling (BIM) are seamlessly integrated through a cutting-edge platform called Autodesk InfraWorks. This innovative tool allows for creating digital representations of the natural world, bridging the gap between virtual design and physical reality. Professionals can build detailed and accurate models using GIS and BIM data within InfraWork, enhancing planning, visualization, and collaboration in various design and construction projects [14]. Integrating Spatial Data (Raster) and BIM Software Infraworks is shown in Figure 13.

Fig. 13. Integrating of Spatial Data (Raster) and BIM Software Infraworks

5.5 Geometry Accuracy Test Results (Horizontal and Vertical)

The method used to test the data's accuracy is based on the Geospatial Information Agency (BIG) Regulation Number 6 of 2018, which provides Accuracy Technical Guidelines for Base Maps. Geometry accuracy tests are applied to orthophoto mosaics to determine their positional accuracy and horizontal error. Meanwhile, vertical accuracy or altitude error is evaluated on Digital Terrain Models (DTM). The procedure for calculating map or image accuracy values is based on Table 2, which specifies RBI map accuracy values by class.

Table 2. Provisions for the value of the RBI map based on class

Accuracy	Class 1	Class 2	Class 3
Horizontal	0.3 mm x scale number	0.6 mm x scale number	0.9 mm x scale number
Vertical	0.5 x contour interval	1.5 x class 1 accuracy	2 x class 1 accuracy

5.6 Horizontal Accuracy

Position accuracy testing refers to the difference in coordinates (X, Y)between the test points on the map and the actual test points on the ground surface [15]. Accuracy measurement uses root mean square error (RMSE). RMSE used to describe accuracy includes a random error, and systematically, this RMSE can be calculated when the coordinate transformation is complete with the formula:

CE90 = 1,5175 x RMSEr   (1)

RMSE horisontal $= \sqrt{D^2}/n$ (2)

Table 3. RMSEr and CE90 Calculation Results

No	Point	(YX)	(YX)^2	DX^2+DY^2
1	ICP1 Jembatan	0.171	0.029	0.040
2	ICP2 Jembatan	-0.515	0.265	0.361
3	ICP3 Lapangan Tenis	-0.367	0.134	0.838
4	ICP5 Jembatan SP	0.025	0.001	0.386
5	ICP6 Jembatan SP	0.506	0.256	0.641
6	ICP7 Ujung Mesjid	-0.281	0.079	0.294
7	ICP8 Ujung Mesjid	-0.654	0.427	0.748
8	ICP9 Batu Lepe	-0.477	0.228	0.377
9	ICP10 Batu Lepe	-0.463	0.214	0.766
10	ICP11 Tepi Laut RSUD	-0.479	0.229	1.137
11	ICP12 Kelenteng 1	-0.086	0.007	0.540
12	ICP13 Kelenteng 2	-0.106	0.011	0.358
13	ICP14 Kelenteng 3	0.012	0.000	0.386
14	ICP15 pelabuhan pelni 1	-0.147	0.022	0.229
15	ICP16 pelabuhan pelni 2	-0.504	0.254	0.654
			Jumlah	7.756
			Rata-rata	0.517
			RMSEr	0.7191
			CE90	**1.0912**

Based on Table 1, it is shown that the horizontal RMSEr value (X, Y) is 0.7191 m, while the accuracy value of the Orthophoto is (Circular Error) CE90, amounting to 1.0912 m. This means that the positional error of the Orthophoto does not exceed that accuracy value with a 90% confidence level obtained using the standard map geometry accuracy

5.7 Vertical Accuracy

RMSEz calculation results were obtained from calculating the difference in the value Z field and Z on DTM. The DEM accuracy value is (Linear Error) LE90 for vertical accuracy, which means that the vertical error does not exceed the accuracy value with a confidence level of 90%.ThisRMSE can be calculated when the coordinate transformation is complete with the formula:

$$LE90 = 1{,}6499 \text{ x } RMSEz \tag{3}$$

$$RMS \text{ vertical} = \sqrt{\frac{(ZDEM - Zcek)^2}{n}} \tag{4}$$

RMSEz and LE90 Calculation Results are shown in Table 4

Based on the table above, the RMSEz value is 2.674 m obtained from the results of the difference between the elevation value (z) of the field and Z on the DTM, while the LE90 value is 4.412 m. The DEM accuracy value is the LE90 (Linear Error) value for vertical accuracy,

which means that the vertical error does not exceed the accuracy value with a 90% confidence level.

After the map accuracy test is carried out, the map accuracy class for a certain map scale can be determined. The accuracy of the map class can be determined by calculating the values of CE90 and LE90, the values of CE90 for horizontal accuracy, and LE90 for vertical accuracy. After knowing the CE90 and LE90 values, the next step is to divide the map accuracy classes at a certain scale, as shown in Table 4.

Table 4. CE90 and LE90 Test Values Scale

No	Accuracy Test	Map Accuracy Test Results CE90 and LE90	Scale Map Accuracy 1:10.000		
			Class 1	Class 2	Class 3
1	Horizontal (CE90)	1.091	2	3	5
2	Vertical (LE90)	4.412	2	3	5

Table 5. RMSEz and LE90 Calculation Results

No	Point	Z DTM (m)	Z field(m)	(DX)	(DX)^2
1	ICP1 Jembatan	17.193	16.772	0.421	0.177
2	ICP2 Jembatan	17.226	16.829	0.397	0.158
3	ICP3 Lapangan Tenis	16.477	16.125	0.352	0.124
4	ICP5 Jembatan SP	16.422	16.269	0.153	0.023
5	ICP6 Jembatan SP	16.551	16.325	0.226	0.051
6	ICP7 Ujung Mesjid	31.318	36.460	-5.142	26.439
7	ICP8 Ujung Mesjid	32.806	36.390	-3.584	12.842
8	ICP9 Batu Lepe	14.871	18.425	-3.554	12.630
9	ICP10 Batu Lepe	15.474	18.416	-2.942	8.658
10	ICP11 Tepi Laut RSUD	13.927	16.227	-2.300	5.289
11	ICP12 Kelenteng 1	26.306	30.081	-3.775	14.251
12	ICP13 Kelenteng 2	26.424	30.022	-3.598	12.946
13	ICP14 Kelenteng 3	26.395	30.085	-3.690	13.614
14	ICP15 pelabuhan pelni 1	15.870	16.149	-0.279	0.078
15	ICP16 pelabuhan pelni 2	16.226	16.304	-0.078	0.006
				Jumlah	107.285
				Rata-rata	7.152
				RMSEz	**2.67438377**
				LE90	**4.412465782**

Based on Table 5, it can be concluded that the results of the horizontal accuracy test (CE90) and the Vertical accuracy test (LE90) are included in the map scale of 1:10,000, with horizontal accuracy fulfilling class 1 and vertical accuracy in class 3.

6 Conclusion

The Fixed Wing UAV has become a revolutionary tool in mapping, significantly contributing to geodesy, geomatics, and civil engineering development. The various advantages of the Fixed Wing UAV make it the optimal choice for various studies. including their resistance to strong winds, long flight duration, and reliable durability. In the research conducted, the data generated by the UAV, be it DEM or Orthophoto, has been proven to meet the accuracy standards set by the Geospatial Information Agency Regulations regarding the accuracy of base maps.

However, as with any research, some drawbacks need attention. One is the absence of official fixed reference points (BM) from the government in the study areas. This study took the BM coordinate reference from the CORS station in Ranai City, Natuna Regency, as a solution. Nonetheless, this poses its challenges, considering that the distance between the study area and the CORS station is approximately 250 km, which affects the accuracy of the coordinates obtained.

Acknowledgments

References

[1] S. A. H. Mohsan, N. Q. H. Othman, Y. Li, M. H. Alsharif, and M. A. Khan, "Unmanned aerial vehicles (UAVs): practical aspects, applications, open challenges, security issues, and future trends," *Intell Serv Robot*, vol. 16, no. 1, pp. 109–137, 2023, doi: 10.1007/s11370-022-00452-4.

[2] H. Liu, Q. Chen, N. Pan, Y. Sun, and Y. Yang, "Three-dimensional mountain complex terrain and heterogeneous multi-UAV cooperative combat mission planning," *IEEE Access*, vol. 8, pp. 197407–197419, 2020.

[3] A. R. Groos, R. Aeschbacher, M. Fischer, N. Kohler, C. Mayer, and A. Senn-Rist, "Accuracy of UAV photogrammetry in glacial and periglacial alpine terrain: a comparison with airborne and terrestrial datasets," *Frontiers in Remote Sensing*, vol. 3, p. 871994, 2022.

[4] A. Alper, "Evaluation of accuracy of dems obtained from uav-point clouds for different topographical areas," *International journal of engineering and geosciences*, vol. 2, no. 3, pp. 110–117, 2017, Accessed: Aug. 15, 2023. [Online]. Available: https://dergipark.org.tr/en/pub/ijeg/issue/31034/329717?publisher=https-www-selcuk-edu-tr-muhendislik-harita-akademik-personel-bilgi-3325-tr

[5] J. A. Gonçalves and R. Henriques, "UAV photogrammetry for topographic monitoring of coastal areas," *ISPRS Journal of Photogrammetry and Remote Sensing*, vol. 104, pp. 101–111, Jun. 2015, doi: 10.1016/j.isprsjprs.2015.02.009.

[6] J. W. Park and D.-J. Yeom, "Method for establishing ground control points to realize UAV-based precision digital maps of earthwork sites," *Journal of Asian Architecture and Building Engineering*, vol. 21, pp. 110–119, 2021, [Online]. Available: https://api.semanticscholar.org/CorpusID:234117252

[7] Z. Guo, "Object Location of Satellite Imagery Under Lacking Ground Control Points," 2003. [Online]. Available: https://api.semanticscholar.org/CorpusID:131512155

[8] L. Barazzetti, R. Brumana, D. Oreni, M. Previtali, and F. Roncoroni, "True-orthophoto generation from UAV images: Implementation of a combined photogrammetric and

computer vision approach," ISPRS Annals of the Photogrammetry, Remote Sensing and Spatial Information Sciences, vol. II–5, pp. 57–63, 2014, doi: 10.5194/isprsannals-II-5-57-2014.

[9] K. Kraus, Photogrammetry: geometry from images and laser scans. Walter de Gruyter, 2011.

[10] S. Manfreda et al., "Assessing the Accuracy of Digital Surface Models Derived from Optical Imagery Acquired with Unmanned Aerial Systems," Drones, vol. null, p. null, 2019, doi: 10.3390/DRONES3010015.

[11] J. J. Yu, D. W. Kim, E. J. Lee, and S. W. Son, "Mid- and Short-Term Monitoring of Sea Cliff Erosion based on Structure-from-Motion (SfM) Photogrammetry: Application of Two Differing Camera Systems for 3D Point Cloud Construction," J Coast Res, vol. 38, pp. 1021–1036, 2022, [Online]. Available: https://api.semanticscholar.org/CorpusID:251980471

[12] E. H. H. Siong, M. F. M. Ariff, and A. F. Razali, "The Application Of Smartphone Based Structure From Motion (Sfm) Photogrammetry In Ground Volume Measurement," The International Archives of the Photogrammetry, Remote Sensing and Spatial Information Sciences, 2023, [Online]. Available: https://api.semanticscholar.org/CorpusID:256682864

[13] K. Yokoo, Y. Kozawa, and T. Sawa, "Theoretical analysis of received optical intensity of underwater image sensor based visible light communications using RGB-LEDs," 2021 24th International Symposium on Wireless Personal Multimedia Communications (WPMC), pp. 1–6, 2021, [Online]. Available: https://api.semanticscholar.org/CorpusID:246660272

[14] A. M. Abd, A. H. Hameed, and B. M. Nsaif, "Documentation of construction project using integration of BIM and GIS technique," Asian Journal of Civil Engineering, vol. 21, no. 7, pp. 1249–1257, 2020, doi: 10.1007/s42107-020-00273-9.

[15] H. Saputra, W. Okcandra, S. Sutikno, and M. Z. Lubis, "Application of Fixed-Wing UAVs to Develop Digital Terrain Model on Coastal Peatland Bengkalis Island," Journal of Applied Geospatial Information, vol. 7, no. 2, pp. 867–874, 2023, Accessed: Aug. 13, 2023. [Online]. Available: https://jurnal.polibatam.ac.id/index.php/JAGI/article/view/4594